LOCAL ATOMIC STRUCTURE STUDY OF CRYSTALLIZATION IN $Fe_{78}Sn_5B_{17}$ AMORPHOUS ALLOY

J. Bednačík[1], I. Mat'ko[2], A. Webb[1] , P. Švec Sr.[2] , P. Švec[2] , D. Janičkovič[2]

[1]Deutsches Elektronen Synchrotron DESY, Notkestrasse 85, D-22603 Hamburg, Germany
[2]Institute of Physics, SAS, Dúbravska cesta 9, 845 11 Bratislava, Slovakia
E-mail: igor.matko@savba.sk

Received 28 April 2015; accepted 05 May 2015

1. Introduction

Fe-B based amorphous alloys represent a model metallic glass system which structure and physical properties are the subject of research over several decades worldwide. Due to their soft magnetic characteristics they have interesting application properties. Their thermodynamic stability, kinetics of crystallization as well as influence of addition of other glass-forming elements into alloy have been widely inspected in hundreds of scientific papers as [1, 2]. Remarkable contribution was the discovery of formation of nanocrystalline phase by controlled crystallization of Fe-B based amorphous alloys containing small addition of specific elements, e.g. Cu, Nb [3]. This discovery raised the interest because of exceptional soft magnetic properties of such a phase. Generally it strongly motivates for a further investigation of the effects of addition of various elements into the Fe-B based alloys.

Sn was selected for our recent investigation for several reasons. Besides atomic radius misfit its low melting temperature is of interest. Moreover Sn represents a Mösbauer active element which opens a perspective to deploy this technique for microstructural analysis. Generally Sn represents a tricky element which hardly dissolves in the solid Fe(Sn) and forms practically no solid solution with boron and so only few results have been published on amorphous or rapidly quenched Fe-Sn-B alloys. In an as-quenched Fe–B based alloy, the critical composition always exists with respect to the elemental proportion of its constituents. Consequently different crystalline phases can grow in hypocritical and hypercritical region [4].

In this paper, local atomic structure is deeply studied using sophisticated structure analysis techniques. Namely hypocritical composition $Fe_{78}Sb_5B_{17}$ was chosen exhibiting two distinct crystallization steps controlled mainly by classical nucleation-and-growth (JMA) kinetics as determined by differential scanning calorimetry (DSC) [5] The study is focused on the first step of crystallization corresponding to nucleation and growth of primary crystalline phase from amorphous matrix. This study is part of a current systematic investigation of the thermodynamic stability and crystallization of the Fe- Sn -B based metallic ribbons [5,6].

2. Experimental

Amorphous ribbon (6mm wide and 30 – 45μm thick), with the nominal composition of $Fe_{78}Sn_5B_{17}$ (at %) was produced by planar flow casting from the temperature 1660K at approximately10^6 Ks^{-1} in air. Ribbons were further thermally treated to receive partially crystalline samples. Namely, based on the inspection of the details of the kinetics of the first crystallization step R1 by DSC (Perkin-Elmer DSC7) [5], each sample was after the continuous-heating ramp with the heating rate 40 °Cmin^{-1} isothermally annealed at the annealing temperature T_a for the annealing time t_a in situ in the DSC instrument and the specific degree of crystallinity (0% to 70%) was obtained. Samples A, B and C isothermally transformed at T_a = 395 °C from the amorphous precursor (t_a = 0, 4.1 and 4.5 min respectively), which at that temperature was in its ferromagnetic state (T_c = 398.4 °C [5]). Samples D and E isothermally transformed at T_a = 405 °C from the already paramagnetic

precursor (t_a = 0 and 2. 5 min respectively).

The microstructure and morphology of the crystallized products was analyzed by transmission electron microscopy (TEM) using conventional JEOL 2000 FX microscope. Samples were prepared by ion-beam milling using a Gatan PIPS machine.

X-ray diffraction (XRD) experiments using high-energy photons were performed at the BW5 wiggler beamline of the DORIS III positron storage ring at DESY/HASYLAB (Hamburg, Germany). The room temperature diffraction patterns were acquired in transmission mode. The energy of the synchrotron radiation was set to 108.9 keV, which corresponds to the wavelength of λ=0.011377 nm. The thin sheet samples were illuminated for 200 s by an incident beam having cross section of 1x1 mm^2. Two-dimensional XRD patterns were collected using an imaging plate detector Perkin Elmer PE1621 (2048×2048 pixels, 200×200 μm^2 pixel size) carefully mounted orthogonal to the X-ray beam. The distance between 2D detector and sample was adjusted to about 43 cm in order to cover high-q range (q=4π sin(θ)/λ) up to 21 $Å^{-1}$. LaB_6 standard was used to calibrate the sample-to-detector distance and tilt of the imaging plate relative to the beam path. About ten independent scans on each sample were averaged to attain optimum counting statistics. Each measurement was followed by background scan, which was later removed from the sample scan. Two-dimensional XRD patterns were integrated to the q-space using the software package FIT2D [7]. The data were then converted to the total structural function, *S(q)*, using standard procedures described in [8]. The integrated data were corrected for polarization, sample absorption, fluorescence contribution and inelastic (Compton) scattering. The total structural factor *S(q)* is obtained from the normalized elastically scattered intensity, $I_e(q)$

$$S(q) = 1 + \frac{I_e(q) - \left[\sum_{i=1}^{n} c_i f_i^2(q)\right]}{\left[\sum_{i=1}^{n} c_i f_i(q)\right]^2} \quad (1)$$

where c_i and $f_i(q)$ are the atomic concentration and atomic scattering factor of the atomic species of type i (i=Fe, Sc), respectively. The corresponding reduced pair distribution function, *G(r)*, can be obtained through a sine Fourier transform:

$$G(r) = 4\pi r\left[\rho(r) - \rho_0\right] = \frac{2}{\pi}\int_0^{q_{max}} q\left(S(q) - 1\right)\sin(rq)dq \quad (2)$$

where $\rho(r)$ and ρ_0 are the *local* and *average* atomic number densities, respectively, and r the radial distance.

The extended X-ray absorption fine structure (EXAFS) measurements were carried out at the bending beamline X1 of the DORIS III positron storage ring at DESY/HASYLAB (Hamburg, Germany). Double-crystal Si(111) and Si(311) fixed exit monochromators were employed. All spectra were collected at room temperature. Samples were measured above the Fe and Sn K absorption edges (7112 eV and 29200 eV) in a transmission. The beam footprint on the sample was 2x1 mm^2. The ionization chambers were filled with inert gases (Ar, Kr) so that the first and second chamber absorbed 10% and 40% of incoming beam intensity, respectively. For every sample the measurement was repeated at least 10 times in order to attain good statistics. The energy calibration was monitored using a reference material (Fe and Sn foils). Fe and Sn foils were measured in transmission mode. The data were processed in the conventional manner using the VIPER program [9].

3. Results and Discussion

The thermodynamic stability as well as the kinetics of the first crystallization step R1 in $Fe_{78}Sn_5B_{17}$ ribbon is well characterized via continuous heating and isothermal DSC curves (Fig.1a, [6]). Microscopic study of the first step of crystallization reveals a formation of

specific nanocrystalline phase consisting of grains of bcc-Fe(Sn) with equiaxed morphology and size up to ~50nm, which are of rather high population embedded in remaining amorphous matrix (Fig.1b). This step generally resembles nucleation and growth of crystalline phase for basic Fe-B based amorphous alloys, however the morphology of grains observed for Fe-Sn-B alloy significantly differs from dendritic one typically observed [1, 2,10].

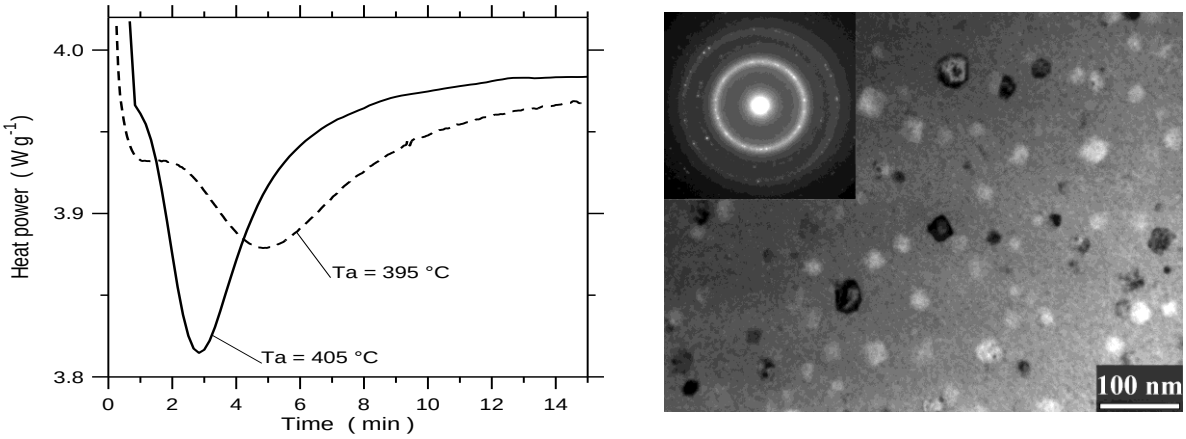

Fig.1 *a) DSC isothermal curves for R1 crystallization step of as-quenched $Fe_{78}Sn_5B_{17}$ ribbon taken at 395 °C (dashed line) and 405 °C (full line). b) Conventional image of microstructure of $Fe_{78}Sb_5B_{17}$ annealed 405°C/2.5min (sample E) Corresponding electron diffraction pattern (inset) confirms bcc-Fe(Sn) structure.*

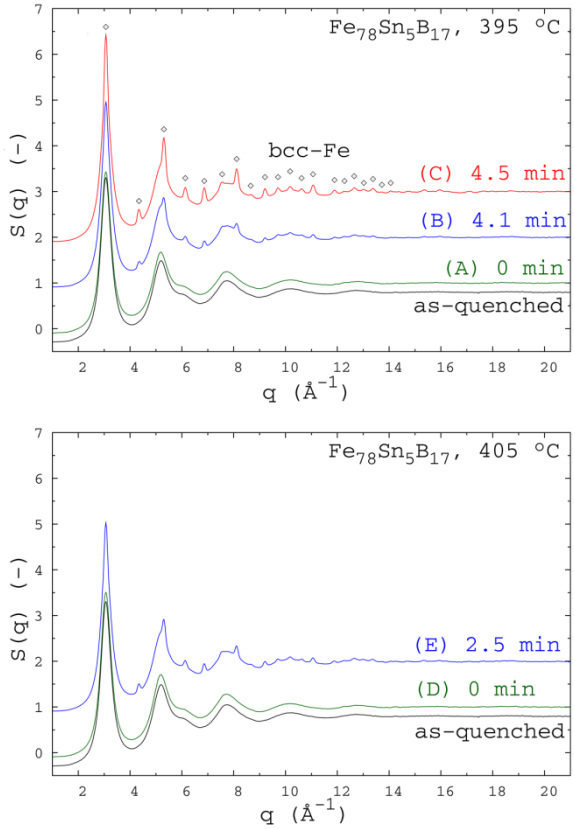

Fig.2 *Structure factors S(q) for $Fe_{78}Sn_5B_{17}$ samples at after annealing at a) 395 °C and b) 405 °C. Small diamonds depict the position of Bragg reflections belonging to bcc-Fe phase. For purposes of better quality all curves are vertically offset.*

XRD patterns reveal that as-quenched sample is fully amorphous and shows characteristic diffuse diffraction pattern without any traces of crystalline phases (Fig.2). When employing heat treatment XRD patterns reveal set of relatively sharp Bragg peaks stemming

from cubic bcc-Fe structure (see Fig.2). However samples are not fully crystallized and exhibit relatively large volume fraction of residual amorphous phase.

In case of a crystalline phase with cubic symmetry one can derive linear relation between Miller indices *hkl* and inverse plane spacing $1/d_{hkl}$ for annealed sample. The slope of corresponding line yields the lattice parameter *a*.. In case of samples C, B and E we obtained values $a = 2.8954 \pm 0.0007$ Å, $a = 2.8952 \pm 0.0013$ Å and $a = 2.8955 \pm 0.0016$ Å, respectively.

To estimate an average grains size from the line broadening in reciprocal space is not possible since the Bragg peaks belonging to cubic phase are still strongly affected by relatively pronounced diffuse signal stemming from amorphous residual. This indirectly suggests that the average grain size can be expected below 10 nm, which is somehow the lowest estimate one can get from the line broadening analysis. Further we calculated reduced pair distribution functions *G(r)* by Fourier transform of structure factors *S(q)* by applying eq.2. Resulting *G(r)* functions are shown in Fig.3. It can be clearly seen from Fig.3 that *G(r)* function corresponding to the as-quenched alloy shows rather broad and rapidly decaying oscillation which is finger print of missing long-range order. Increasing the level of crystallized fraction has significant impact on the shape of *G(r)* which reveals appearance of rather sharp oscillations, visible up to much longer r-distances. This is directly connected with formation of long-range order correlations implying an increase of the average grain size. So one can use the upper limit of *r*, actually the distance up to which are the oscillations in *G(r)* still above the noise level, as an estimate for the average grain size. In case of the samples C and B oscillations are visible up to r_{max}=4.5 nm which corresponds to the average grain size. As a consequence of nanoparticles random distribution (there is no preferred orientation) inter-particle correlations are effectively zero and therefore no correlations are revealed on *G(r)* functions above *r*=4.5 nm.

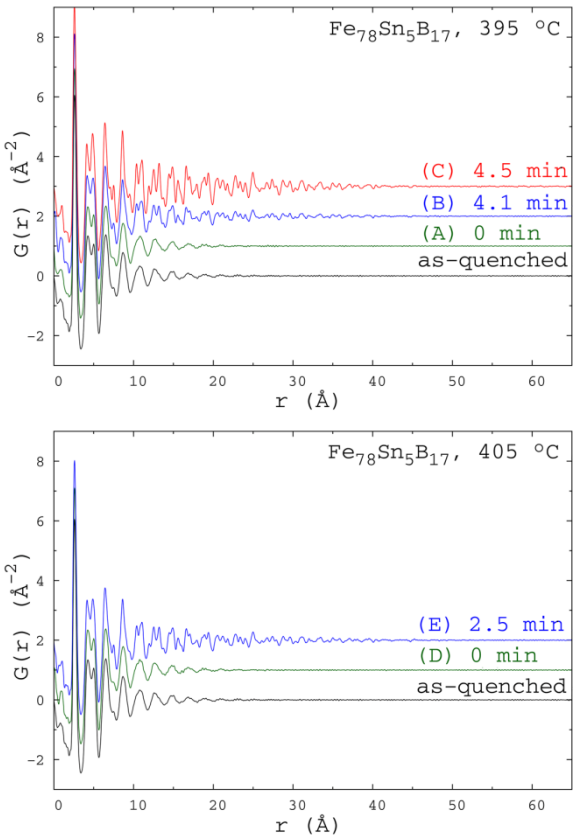

Fig.3 *Reduced pair distribution functions, G(r), for $Fe_{78}Sn_5B_{17}$ samples after annealing at a) 395 °C and b) 405 °C. For purposes of better quality all curves are vertically offset.*

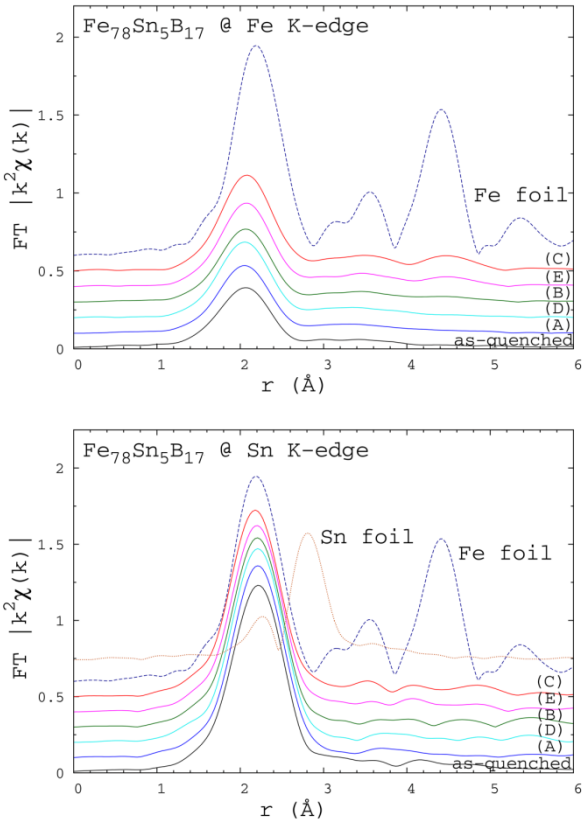

Fig.4 *Fourier transform of k^2 weighted EXAFS signal χ for $Fe_{78}Sn_5B_{17}$ samples after annealing at a) 395 °C and b) 405 °C. Obtained distribution functions are not phase corrected. For purposes of better quality all distribution functions are vertically offset. Dashed and dotted lines correspond to measurements on calibration Fe and Sn foils, respectively.*

Figure 4 shows Fourier transform of k^2 weighted EXAFS χ signals at different stages of thermal treatment. In case of X-ray absorption measurements performed at the Fe K-edge (Fig.4a), corresponding distribution curves show only one broad peak. Its position perfectly matches the first coordination sphere for Fe-bcc. With increasing degree of crystallinity one may observe formation of additional peaks associated with higher coordination shells of Fe-bcc structure. Distribution functions obtained from X-ray absorption measurements performed at the Sn K-edge (Fig.4b) show only one broad peak which position perfectly agrees with the position of the broad peak observed in case of measurements at the Fe K-edge. This suggests that Fe and Sn have similar environments. It also indicates that there is no significant clustering of Sn atoms during thermal treatment and Sn atoms most probably substitute some of Fe atoms in Fe-bcc structure.

High-resolution TEM analysis shows rather faulted inner structure of Fe(Sn) grains [6]. This should be a consequence of incorporation of Sn atoms into Fe crystalline lattice as proposed by EXAFS studies and supported also by fact that no clustering of Sn atoms was observed. An average size of ordered region (corresponding to subgrain) could be estimated from microscopic images to ~5 nm, which correlates with average grains size value determined by XRD measurements. So the bcc-Fe(Sn) grains can be interpreted as clusters of subgrains of size typical to nanocrystalline material (~5 nm). This specific nanocrystalline phase remains present up to higher stage of second crystallization step which corresponds to transformation of remaining amorphous phase to iron borides [6].

Already unusual details in the kinetics of the R1 crystallization step in $Fe_{78}Sn_5B_{17}$ have been reported in [5]. Namely at first, it is controlled by the JMA kinetic law with $n_1 = 2$ in the

isothermal case or n_1 = 1.5 in the continuous heating regime and simultaneously at the advanced stages, it dramatically decays to $n_1 < 1$ suggesting finally the grain-growth-like kinetics with $m_1 \sim 0.8$. Thus the formation of the bcc-Fe(Sn) grains principally reveals the formation of spherulites in Fe-Si-B glasses (n_1 = 2.5 [10]) and nanocrystals in the FINEMETs [11]. The actual XRD measurements, namely the observation of the bcc-Fe(Sn) grains being in fact the clusters of nanometer size subgrains (~5 nm).

4. Conclusions

The first step of crystallization of Fe–Sn–B alloy for hypocritical composition is characterized by JMA kinetics controlled formation of bcc-Fe(Sn) specific nanocrystalline phase with grain size up to ~50nm and relatively high thermal stability. There is no significant clustering of Sn atoms during thermal treatment and Sn atoms most probably substitute some of Fe atoms in emerging Fe-bcc structure. The consequence of Sn incorporation is a rather faulted inner structure of bcc-Fe(Sn) grains which can be interpreted as clusters of subgrains of size typical to nanocrystalline material (~5 nm).

Acknowledgement

This work was supported by the projects VEGA 2/0189/14, APVV-0492-11, APVV-0460-12 and by the CEX FUNMAT.

References:

[1] A.L.Greer: *Acta Metall.*, **30**, 171 (1982).
[2] E. Illeková, I. Maťko, P. Duhaj, F.-A. Kuhnast: *J. Mater. Sci.*, **32**, 4645 (1997).
[3] Y.Yoshizawa, S.Oguma, K.Yamaguchi: *J. Appl. Phys,*. **64**, 6044 (1988).
[4] U.Köster,in:B.L.Mordike(Ed.): Phase Transformations in Crystalline and Amorphous Alloys, DGM,Oberursel, Germany (1983).
[5] E. Illeková, I. Maťko, P. Švec, P. Švec Jr., D. Janičkovič: *J. Alloys and Comp.* **509S**, S46 (2011).
[6] I. Maťko, E. Illeková, P. Švec Sr., P. Švec, D. Janičkovič, V. Vodárek: *J. Alloys and Comp.* **615**, S462 (2014).
[7] A. P. Hammersley, S. O. Svensson, M. Hanfland, A. N. Fitch, and D. Häusermann: *High Press. Res.,* **14,** 235 (1996).
[8] T. Egami and S. J. L. Billinge: Underneath the Bragg Peaks: Structural analysis of complex materials, Pergamon Press, Elsevier, Oxford, England (2003).
[9] K.V. Klementev: *J. Phys. D: Appl. Phys.* **34**, 209 (2001).
[10] I. Maťko, E. Illeková, P. Švec, P. Duhaj: *Mat. Sci. Eng.*, **A225,** 145 (1997).
[11] E. Illeková: *Thermochim. Acta*, **387** 47 (2002).